Multi-frequency acoustic inversion derived from a broad and shifting grain size distribution using "off-the-shelf" acoustic Doppler current profilers

D.W. Haught
Simon Fraser University, BC, Canada

J.G. Venditti
Simon Fraser University, BC, Canada

S.A. Wright
U.S. Geological Survey, California Water Science Center

M. Church
University of British Columbia, BC, Canada

ABSTRACT: Suspended sediment particle size in rivers is of great interest due to its influence on riverine and coastal morphology, socio-economic viability, and ecological health and restoration. Prediction of suspended sediment transport from hydraulics remains a stubbornly difficult problem, particularly for the washload component, which is controlled by sediment supply from the drainage basin. This has led to a number of methods for continuously monitoring suspended sediment concentration and mean particle size, the most popular currently being hydroacoustic methods. Here, we explore the possibility of using theoretical inversion of the sonar equation to derive an estimate of mean particle size, relative standard deviation of the grain size distribution (GSD), and concentration. Instruments were deployed in the sand-bedded reach of the Fraser River, British Columbia. We use 298 bottle samples collected in the acoustic beams to test acoustics signal inversion methods. We present results from an acoustic inversion where multiple water samples were collected and analyzed.

1 INTRODUCTION

Over the last several decades the use of "off-the-shelf" acoustic Doppler current profilers (ADCPs) has become a common tool in river and oceanic hydraulic observations. They can reliably produce velocity and discharge when calibrated. Additionally, these instruments resist fouling and deliver higher spatial and temporal resolution observations. Sedimentologist's have become increasingly interested in their use due to the possibility of acoustically inverting the returned backscatter signal to estimate sediment concentration and mean particle size. The coupling of these sedimentological characteristics with the velocity and discharge data provides the additional advantage of obtaining an estimate of sediment flux, both total and, potentially, size specific.

Prediction of suspended sediment flux from hydraulics remains a stubbornly difficult problem, particularly for the washload component which is controlled by sediment supply from the drainage basin. Traditional methods, such as relations produced by sediment rating curves, can produce significant error (Walling, 1977), especially when hysteretic relations are present. In the Fraser River (British Columbia, Canada), where this study takes place, hysteretic rating curves occur (McLean et al. 1999a) and can contribute to inaccurate sediment load estimations.

The theory of multi-frequency acoustic inversions has been developed over the last three decades (Hay, 1991; Crawford and Hay 1993; Holdaway and Thorne, 1999; Thorne and Hardcastle, 1997; Thosteson and Hanes, 1998) and reviewed more recently (see recent reviews by Thorne and Hanes, 2002; Thorne and Hurther, 2014). These studies have primarily taken place at the small scale (meters) (Sheng and Hay, 1988; Thorne and Campbell, 1992; Thosteson and Hanes, 1998; Moate and Thorne, 2009) or in the near-shore environment where grain size distributions (GSD) are unimodal and narrow or in laboratories where the GSD is purposely constrained.

More recently, multi-frequency acoustic inversion investigations have moved into estuarine (Thorne et al., 1994) and riverine environments (Guerrero et al., 2013; Moore et al. 2012, 2013) where grain size distributions vary due to differing sources and flocculation. This has led to laboratory studies that have examined acoustic response to suspensions with different particle shape (Thorne et al., 1995a; Richards 2003; Thorne and Buckingham, 2004), mixed mineralogy (Schaafsma and Hay, 1997; Moate and Thorne, 2011, 2013), broad and bimodal size distributions (Moate and Thorne, 2009), and, more recently, flocculated aggregates (MacDonald et al., 2013; Thorne et al., 2014).

These studies have shown that acoustic signals, either through backscattering or attenuation, are significantly influenced by the median size of the particle, concentration or number of particles in suspension, shape and mineralogy of the particles in suspension,

and the GSD breadth. Moate and Thorne (2009) have shown how variability in the GSD can perpetuate error through the inversion, resulting in error in both the estimated median grain diameter and/or the mass concentration.

Previous application of acoustic inversion techniques in riverine environments have assumed constant particle mineralogy and shape of the GSD, which was justified because sediment sources were partly controlled by the presence of large-scale dams that filter some of the variability in sediment size (e.g. Moore et al. 2012, 2013). Here we apply the acoustic inversion methods in a somewhat more challenging riverine environment where sediment sources vary through the annual freshet, causing changes in particle concentration, size, size distribution, minerology, and shape (McLean et al. 1999a; 1999b; Haught et al., 2014).

In this paper we seek to determine: How well can we predict mass concentration and grain-size using existing inversion techniques in a system where we know there are changes in mass concentration, grain size and grainsize distribution? We use a mixed implicit/explicit acoustic inversion method that accounts for a drifting GSD.

2 METHODS

2.1 *Acoustic theory*

2.1.1 *Acoustic Inversion and scattering*

Commercial acoustic Doppler current profilers return a backscatter signal that reflects the size and number of scatterers in Intensity (E) with units of counts. These units are converted to acoustic intensity (in decibels) through:

$$I_{db} = (E - E_{noise}) * k_c \quad (1)$$

where the acoustic intensity, I_{db}, is in decibels. E_{noise} is the echo noise floor in counts and k_c is calculated as:

$$k_c = \frac{127.3}{T_e + 273} \quad (2)$$

where T_e is the temperature given by the instrument in degrees Celsius. E_{noise} is the detection threshold (DT) which is the value (in counts) that is given by the instrument when several pings are run in air (Moore et al., 2012; Teledyne RDI, 2008). The acoustic intensity is then transformed into linear form to find the acoustic pressure, P^2_{rms}:

$$\frac{P^2_{rms}}{P^2_{ref}} = 10^{\frac{I_{db}}{10}} \quad (3)$$

where P^2_{ref} is the reference pressure which is equal to 1 μPa. The pressure received from the ADCP can be related to concentration and particle size as:

$$P^2_{rms} = P_o^2 r_o T_v R \frac{k_t^2 k_s^2}{r^2 \psi^2} M e^{-4r\alpha} \quad (4)$$

where P_o and r_o are components of the source level (SL in decibel form: see below) and are defined as the reference pressure and reference range, r_o=1 m. T_v and R_t are the voltage transfer function of the system and transducer receive sensitivity, respectively. M is the mass concentration (kg/m^3), r is the range, α is the attenuation of the signal due to fluid, viscous shear, and scattering losses (α_w+α_s). ψ is the near-field correction (Downing, 1995), k_t is an instrument constant while k_s reflects acoustic characteristics relative to particle size. k_t can be defined as:

$$k_t^2 = T_v R_t \frac{3\tau c}{16} \left(\frac{0.96}{k a_t}\right)^2 \quad (5)$$

where a_t is the transducer radius, c is the celerity of sound in water, k is the wavenumber, and τ is the pulse duration. Because all parameters in Equation 5 except T_v and R are given by the instrument it is logical to combine the two unknowns into the source level, which for commercial ADCPs is also unknown:

$$SL = T_v R_t \frac{P_0^2 r_0^2}{P_{ref}^2} \quad (6)$$

The source level has also been described by Urick (1975) and reflects $P_o r_o / P_{ref}$ in decibel form as:

$$SL = 170.8 + 10 log_{10}(WA) + DI \quad (7)$$

where DI is the directivity index and is equal to 10*log10($2\pi a_t \lambda^{-1}$) in decibel form, and WA is the effective transmit power in watts. λ is the acoustic wavelength in meters, which is equal to the ratio of the celerity of sound in water to acoustic frequency (Hz). Table 1 gives values of both Equation 6 and 7 for comparison, along with parameters suggested by Teledyne RDI©.

Table 1. Acoustic parameters used in the acoustic inversion. Note that the values of WA were recommended from Teledyne RDI and are approximations. Where the overbar represents mean values over all collected samples.

Instrument Frequency	$\overline{SL}$ **(dB) Eq. 7**	$\overline{SLTvR}$ **(dB) Eq.6**	$\overline{k_t}$ **Eq.22**	a_t **(m)**	**WA (Watt)**	$\overline{f_o}$ **Eq. 23**
1200	197	187	9.7E7	0.051	3.2	0.01
600	202	199	5.7E8	0.095	9.6	0.003
300	202	205	1.9E9	0.128	16.6	0.001

The term k_s in Equation 4 reflects the scattering properties of the particles in suspension and is therefore a function of particle radius, a:

$$k_s^2 = \frac{\int_0^\infty a^2 f_o^2 n(a) da}{\rho \int_0^\infty a^3 n(a) da} \quad (8)$$

where *n(a)* is the probability distribution function (PDF) by number of particles, ρ is the particle density, and f_o is the backscatter form function which can be described theoretically as:

$$f_o(x) = \frac{2}{ix} \sum_{n=0}^{\infty} (2n+1)(-1)^2 b_n \quad (9)$$

where b_n has been defined by Gaunard and Ubrell (1983) and is a function of the suspended particle properties. For this work we use the heuristically derived empirical form function defined by Thorne and Meral (2008) as:

$$f_o(x) = x^2 \left(1 - 0.35e^{-\left(\frac{x-1.5}{0.7}\right)^2}\right) * \left(1 + 0.5e^{-\left(\frac{x-1.8}{2.2}\right)^2}\right) * (1 + 0.9x^2)^{-1} \quad (10)$$

where x=*ka*. Rearranging Equation 4 leads to the inversion which solves for mass concentration and has the form:

$$M = \frac{P_{rms}^2 r^2 \psi^2}{k_t^2 k_s^2} e^{4r\alpha} \quad (11)$$

where the attenuation, α, is a function of mass concentration and attenuation losses. The grain size distributions found in the Fraser River tend to be log-normal, though bi-modal distributions are also observed. For this acoustic inversion we define *n(a)* as:

$$v(a) = \frac{1}{a\sigma\sqrt{2\pi}} \exp\left(-\frac{(\ln a - \ln a_g)^2}{2\sigma^2}\right) \quad (12)$$

where *v(a)* is the particle density function (PDF) by volume and the conversion of *n(a)* to *v(a)* is described thoroughly in Moore et al. (2013). Here the particle radius, *a*, is varied from 10^{-2} to 750 microns through the inversion, a_g is the geometric mean particle radius, and σ is the relative standard deviation and is defined as:

$$\sigma = \sqrt{ln(\sigma_o^2 + 1)} \quad (13)$$

and

$$\sigma_o = \frac{\sigma_{arith}}{a_{arith}} \quad (14)$$

where σ_{arith} and a_{arith} are the arithmetic standard deviation and mean particle radius, respectively.

2.1.2 *Attenuation*

Flammer (1962) shows that attenuation of sound from sediment can be attributed to three loss mechanisms: the scattering of sound by a particle as a function of the ratio of acoustic wavelength to particle circumference, $\alpha_{s,\,scatt}$, energy loss due to viscous shear, which is a function of particle density and surface area, $\alpha_{s,visc}$, and heat loss due to conduction. Heat loss is significantly less in magnitude than scattering and viscous loss and is generally neglected. Here sediment attenuation is given by:

$$\alpha_s = \alpha_{s,visc} + \alpha_{s,scatt} = M\langle\zeta_{visc}\rangle + M\langle\zeta_{scatt}\rangle \quad (15)$$

where $\alpha_{s,visc}$ is the attenuation of sound due to viscous losses and $\alpha_{s,scatt}$ is the attenuation of sound due to scattering losses. ζ_{visc} and ζ_{scatt} are the viscous and scattering attenuation coefficients averaged over the grain size distribution, which is indicated by the brackets, < >. The scattering attenuation coefficient has been described empirically by Thorne and Meral (2008) as:

$$\langle\zeta_{scatt}\rangle = \frac{3\int_0^\infty a^3 \chi n(a) da}{4\rho \int_0^\infty a^3 n(a) da} \quad (16)$$

where χ has been empirically described by Thorne and Merel (2008) as:

$$\chi = \frac{0.29x^4}{0.95 + 1.28x^2 + 0.25x^4} \quad (17)$$

The viscous attenuation coefficient can be described by Urick (1948) as:

$$\langle\alpha_{s,visc}\rangle = M\frac{\int_0^\infty \zeta_{visc}(a) a^3 n(a) da}{\int_0^\infty a^3 n(a) da} \quad (18)$$

and,

$$\langle\zeta_{visc}\rangle = \frac{k(G-1)^2}{2\rho_s}\left[\frac{s}{s^2 + (G+\delta)^2}\right] \quad (19)$$

where:

$$s = \frac{9}{4ba}\left[1 + \frac{1}{ba}\right] \quad (20)$$

and,

$$G = \frac{\rho}{\rho_w};\ \delta = \frac{1}{2}\left[1 + \frac{9}{2ba}\right];\ b = \sqrt{\frac{\omega}{2v}} \quad (21)$$

where ρ_w is fluid density, ν is kinematic viscosity of water, and ω is the angular frequency.

2.2 *Suspended sediment samples and acoustic instrument setup*

Field observations are from the Fraser River, at Mission (Water Survey of Canada (WSC) station no. 08MH024), BC, approximately 85 km from the river

mouth at the Strait of Georgia. Here, the Fraser is constrained to a single ~550 m wide channel carrying runoff from the 228,000 km^2 basin. This section provides an ideal location to measure the input of flow and sediment to the increasingly industrialized Fraser Estuary and Delta. The runoff pattern is dominated annually by the spring snowmelt in May-June initiating a freshet in late May, June and early July. The mean annual flow at Mission is 3410 m^3/s and the mean annual flood is 9790 m^3/s. McLean at al. (1999a) found that on average 17 million tonnes per year (Mt a^{-1}) of sediment moved past Mission, BC using WSC 1965-1986 data. About one third, 6.1x10^6 Mt a^{-1}, is suspended sand and half of that (3.0 Mt a^{-1}), is sand finer than 0.177 mm (McLean *et al.*, 1999a), which is washload (suspended material present in amounts >10% of the bed material).

Three horizontally oriented acoustic Doppler current meters (Teledyne RDI, USA) were mounted on the Mission Harbour Authority dock just upstream of the Mission railway bridge. The instruments have acoustic frequencies of 307.2, 614.4 and 1228.8 kHz (referred to as 300, 600, 1200 hereafter). The H-ADCPs were set to collect data for one minute, then rest for one minute before another started, equating to 6 minute intervals for each H-ADCP. The range used in the analysis is limited to the maximum distance of the 1200 kHz ADCP (~36 m) because it has the shortest maximum distance and the multi-frequency approach relies on spatially coupled signals.

Sediment sampling campaigns were undertaken to calibrate and evaluate acoustically derived surrogate suspended sediment concentrations. The suspended sediment samplings consisted of six campaigns in 2012, eight in 2013 and eleven in 2014 and were designed to capture a wide variety of flows through the annual Fraser River freshet.

A 200-pound USGS P-63 sampler, deployed from a vessel using a motorized USGS E-reel, was used to collect point-integrated, isokinetic suspended sediment samples. A series of 'in-beam' (IB) samples was taken at calculated distances and depths across the channel to align with the ADCP beams. The locations ranged from 6 to 250 m from the ADCPs. Distances were selected such that there were roughly 5 equally-spaced samples in each of the three acoustic beams. Each of the suspended sediment samples was processed in the Simon Fraser University (SFU) River Dynamics Lab using a LISST-100 (Sequoia Scientific, USA) instrument that uses laser diffraction to calculate the fractional grain size distribution (GSD) between 2 and 350 microns. Sediment mass concentration was also obtained using the traditional filter (0.45 μm) method after the sample passed through the LISST-100.

Additionally, four samples were collected using a modified P-61 on June 19 and July 22, 2014 at in-beam 18 and 48 (IB18 and IB48). The modified P-61 pumps the sample to the surface through a tube connected to the inside nozzle at flow rates that match the velocity at the nozzle. The velocity at the nozzle is determined by a down-facing ADCP, of which the nearest bin to the desired depth is used. This modification allowed large sediment samples to be collected at isokinetic rates. Samples were then decanted, split and run through both the LISST-100 and a Beckman Coulter LS 13 320 Laser Diffraction Particle Size Analyzer (Coulter, USA) which has a larger range than the LISST-100 (0.4-2000 microns), but utilizes similar theory to obtain particle diameter.

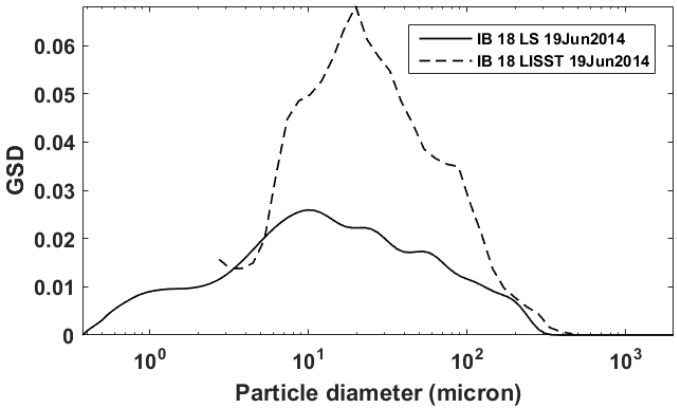

Figure 1. Example of grain size distributions for samples collected with the modified P-61 sediment sampler and run through a LS 13 320 (LS) and the comparative samples run through the LISST-100 (LISST).

3 RESULTS

3.1 *In-situ samples*

From 2012-2014, 298 samples were collected and processed resulting in median values of 84 mg/L, 28 μm, and 2.6 for mass concentration, geometric mean particle diameter and geometric standard deviation, respectively. The GSD geometric standard deviation of the samples collected is broad and ranges from 1.9 to 3.8. Though the results from the LISST-100 suggest that the particles in suspension are primarily medium silt, the comparison between the larger sediment samples collected with the modified P-61 and run through both the LISST and a LS 13 320 suggest that the LISST is missing the lower end of the GSD, which is primarily clay and some very fine silt (Figure 1).

Figure 1 shows the GSD for both size distribution analyses allowing for an estimate of the error produced by the instrument limitations of the LISST-100. It is clear from this figure that the LISST-100 is missing the fine silt and clay portion of the GSD. Figure 2 shows how the LISST measured GSD changes over the three years of sample collection averaged over the rising, peak, falling and low flow periods of the hydrograph. It can be seen that the GSD changes from unimodal during low flow periods to a bi-modal distribution during the freshet, with the GSD at its broadest during peak flow. The fact that the LISST-

100 is missing the clay portion of the GSD suggest that the GSD may be broader and the median diameter smaller than has been measured by the LISST analysis.

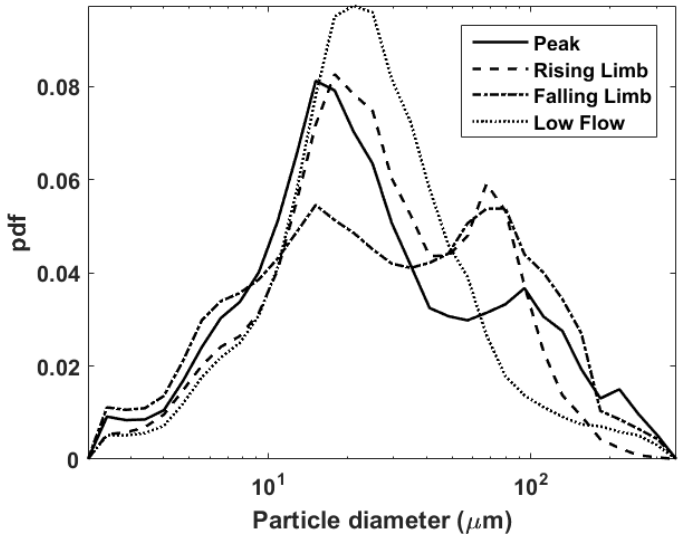

Figure 2. Grain size distributions for four samples collected from 2012-2014 over the rising, peak, falling, and low flow components of the hydrograph.

3.2 *Backscattering form function and k_t in response to broad grain size distributions*

To compute the instrument constant, k_t, we utilized the method described by Betteridge et. al. (2008), where the rearrangement of Equation 4 results in:

$$k_t = \frac{P_{rms}\psi r}{k_s M^{1/2}} e^{4r\alpha} \tag{22}$$

Note the difference from Betteridge et. al. (2008), who use V_{rms} in Equation 6, since they know the values of P_o and therefore solve for T_vR. For these commercial instruments the value of P_o is unknown and can only be estimated by Equation 7, as is given in Table 1. Table 1 gives the average k_t over all 298 samples. In an attempt to reduce the influence of sediment attenuation, suspended sediment samples outside of 20 meters from the ADCPs and greater than 50 mg/L were not used, though attenuation is accounted for in Equation 22. Mean values were computed once outliers were removed. Outliers were defined as any value greater than two standard deviations from the initial mean.

Once k_t is solved for each instrument one can solve for f_o using the theoretical values of χ and attenuation from fluid, viscous shear, and scattering computed from the measured GSD and mass concentration using Equations 15 through 21. The backscattered form function can be computed by:

$$f_o = \frac{P_{rms}\psi r\sqrt{a\rho}}{k_s M^{1/2}} e^{4r\alpha} \tag{23}$$

The average results from Equation 23 are given in Figure 3 and Table 1, which shows that results from all three frequencies give higher values than those modeled by Equation 10. This occurrence has been investigated by Moate and Thorne (2009), who show how broad grain size distributions can shift the backscattering form function in both the Rayleigh scattering regime (x<1) and geometric scattering regime (x>1). The cause of the divergence from Equation 10 could also be variability in particle shape or density (Moate and Thorne 2011; 2013). Moate and Thorne (2009) also note that the variation seen in the results found in Figure 3 may be attributed to variability found in k_t and in χ. Though the variability in χ is difficult to prevent since the model is based on average values (Eq. 17), with the median sediment size found in suspension (~25μm) it is more likely that underestimates of viscous shear contribute more to the variability found in Figure 3.

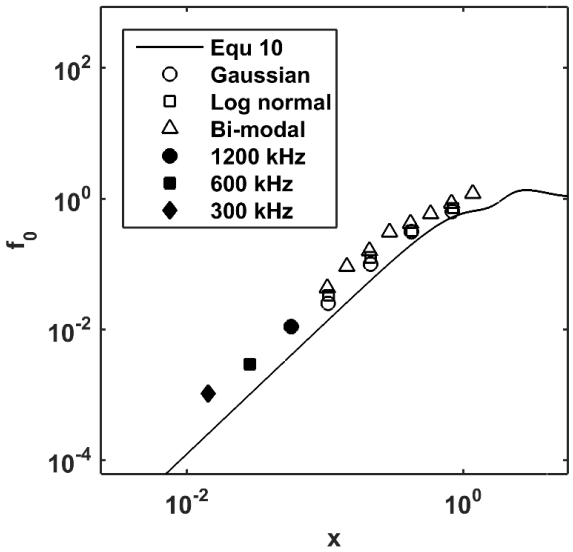

Figure 3. Average values of f_o computed from Equation 20 and data from Moate and Thorne (2009) for their (○) Gaussian distribution, (□) log normal distribution, and (Δ) bi-modal distribution included for comparison.

3.3 *Acoustic inversion*

In order to invert acoustic signals into estimates of concentration using Equation 11, a three step process is used. First, particle radius is found by using the preset range and distribution (described above in Eq. 12-14) to solve:

$$\varepsilon_i = \left[\frac{P_{rms} r\psi}{k_s k_t}\right]^2 e^{4r(\langle\zeta_{visc}\rangle+\langle\zeta_{scatt}\rangle)} \tag{24}$$

where Equation 24 is in a form similar to Equation 11, but excludes mass concentration, allowing for the sensitivity to be associated to changes in particle radius. Here the subscript, *i*, represents each frequency. The ratio of each frequency is computed as:

$$\epsilon_{i,j} = \frac{\varepsilon_i}{\varepsilon_j} \tag{25}$$

where i and j are two different frequencies and are minimized between all three pairs by:

$$Min(\epsilon_{i,j}) = \frac{std(\epsilon_{\frac{1200}{600},\frac{600}{300},\frac{1200}{300}})}{\langle \epsilon_{\frac{1200}{600},\frac{600}{300},\frac{1200}{300}} \rangle} \quad (26)$$

which produces an acoustic profile for each range, r, that is minimized at the estimate of particle radius shown in Figure 4.

Figure 4 A and B show that there are multiple minimizations across the particle range used. For this analysis the second minimization was used throughout. At times, in the near-field, no second minimization occurred and the third minimization was given (Figure 4B).

Once particle radius is estimated, the second step in estimating the relative standard deviation (in log-normal form), given in Equation 13, is computed using a method similar to particle radius. Particle radius is held constant (using the particle radius estimated above) while Equations 24-26 are solved for a range of relative standard deviations between 0.25 to 1.5 at 0.05 increments. Again, the minimization is found for each profile at each range, providing both a mean across the range and a range-specific value.

Lastly, an initial estimate of mass concentration is computed by using the estimates of particle radius and relative standard deviation in equations 8, 11, and 15-21. Because mass concentration is on both the RHS and LHS of Equation 11 via Equation 15, to solve for mass concentration requires iterative computations. To accomplish this, we use the method described in Thorne and Hurther (2014) and references therein. Once the initial estimate of mass concentration is made for the range bin closest to the ADCP's, the rest of the range bins are computed using the explicit method described by Thosteson and Hanes (1998) utilizing the estimated particle radius and relative standard deviation for each range bin.

Table 2. Results of the acoustic inversion and those from the LISST-100 (LISST) and LS 13 320 (LS) for the sample day June 19, 2014 at in-beam 18 meters from the ADCPs.

	D_{50} (μm)	Spatially averaged σ	M (mg/L)
Acoustically derived	5.9	0.95	155.4
Measured by LISST	16.6	1.2	n/a
Measured by LS	12.7	1.4	n/a
Mass Concentration by filter	n/a	n/a	71.9

Table 2 gives the results for this acoustic inversion method for June 19, 2014. Mass concentration, particle diameter and spatially-averaged relative standard deviation are compared to LISST-100 measurements. Results show that particle diameter is underestimated by the acoustic inversion compared to the LISST-100 estimates. When comparing LS 13 320 results to those of LISST-100 results, an underestimation is expected because of the limitation of the LISST-100 grain size range. This consequence has ramifications on both the inversion results in Table 2 and the accuracy of the estimates of attenuation, backscattering and possibly the instrument constant used in the inversion. Given the described overestimation by the LISST-100, results in Table 2 still suggests that the acoustic inversion is underestimated when using LS 13 320 results. Results, again, suggests that the inversion produces an underestimated relative standard deviation of the GSD. The underestimation is expected by the LISST-100 due to the lack of account of the clay portion of the GSD. Lastly, the concentration given by the inversion is overestimated by approximately twofold when comparing the result to the measured and filtered mass concentration.

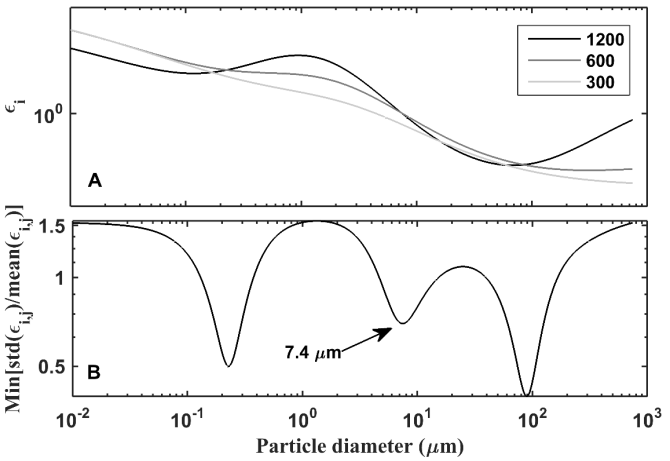

Figure 4. Method for determining particle radius showing the results of (A) Equation 24 and (B) Equation 26. The second minimization was used throughout the analysis as the first and third result in clear under- and over- estimates, respectively. Acoustic inversion is from June 19, 2014 for the sample location 18 meters from the three ADCP's. LISST-100 and LS 13 320 results are from Figure 1, as they were coupled by location and sampling day.

4 DISCUSSION AND CONCLUSION

Unlike the typical suspended sediment distributions found in near-shore tidal suspensions (Thorne et al. 2007) and in river environments where suspended sediment distributions may be more narrow and unimodal due to an upstream sediment supply control (e.g. Moore et al., 2013) the sediments in the Fraser River have a broad and changing GSD. Because of stable GSDs in previous studies, current acoustic inversion methods have neglected the possibility of a shifting GSD by treating the standard deviation used in the modeling of the distribution in Equations 8, 13, and 15 as a constant. Moate and Thorne (2009) have shown that when the standard deviation of the GSD

in either underestimated or overestimated, an inverse response can occur in the estimate of concentration and particle radius. This work has presented an acoustic inversion that can account for a shifting and broad GSD by estimating the relative standard deviation, in addition to the particle radius and concentration.

The mixed implicit/explicit acoustic inversion method, similar to Thosteson and Hanes (1998), presented here provides a means to estimate both the median particle diameter and GSD standard deviation, allowing for an estimate of mass concentration. This method was able to produce good results when compared to measured sediment properties. Results give a good comparable values that are on the same order of magnitude. The underestimated particle diameter was expected due to instrument limitations. The relative standard deviation of the GSD was underestimated and likely lead to an overestimate of concentration. These results are similar to trends found in models simulated in Moate and Thorne (2009, Figure 10), suggesting that the underestimation of the relative standard deviation may be the cause of the underestimated particle diameter and the overestimated concentration.

Acoustically derived mass concentrations appear to be overestimated compared to measured samples using a point-integrated (USGS P-63) sampler (Table 2). This overestimation may be the most significant indicator of error in the acoustic inversion as LISST-100 data were shown to overestimate particle diameter and underestimate relative standard deviation of the GSD. With that said, both Topping et al. (2011) and Gitto (2015) have shown that short sampling durations (with the P-63, ~45 s) may lead to substantial error in concentration estimates, suggesting that there could be error in the measured mass concentrations and GSDs as well.

Transient deviation in GSD in the Fraser River presents a challenge when using a three frequency approach to invert the acoustic signal. Error in the estimate of particle diameter and/or relative standard deviation, as shown by Moate and Thorne (2009), can result in error in concentration estimates. To reduce this error, it may be necessary to add another frequency to the acoustic inversion in environments similar to that of the Fraser River. Additionally, the use of a bi-modal distribution, instead of a unimodal distribution (Eq. 12) in the inversion method may be more appropriate, though making the method of estimating the relative standard deviation more complicated.

A four frequency approach would provide a more accurate estimate of mass concentration and median particle diameter as it would benefit the mathematical accuracy of determinations of the three unknowns (M, a_s, σ_d). A fourth frequency will allow for the non-linear system of equations to solve for the three unknowns (Thosteson and Hanes, 1998). External sources of knowledge (i.e. discharge) that can be related to the GSD standard deviation may work as well (this possibility is another beneficial aspect of the ADCPs providing velocity and discharge). Additionally, mixed mineralogy and particle shape affects may contribute to the error in the results. This aspect warrants investigation and would likely require more of the unknowns to be accounted for, further stressing the use of four frequencies in environments similar to the Fraser River.

5 REFERENCES

Betteridge, K.F.E., Thorne, P.D., Cooke, R.D., 2008. Calibrating multi-frequency acoustic backscatter systems for studying near-bed suspended sediment transport processes. Cont. Shelf Res. 28,227–235.

Church, M. 2007. Review of the lower Fraser River sediment budget: final report. Report to Fraser River Estuary Management Program, 26 July, 2007: 24pp.

Crawford, A.M. and Hay, A.E., 1993. Determining suspended sand size and concentration from multifrequency acoustic backscatter. J. Acoust. Soc. Am. 94(6), 3312-3324.

Downing, A., Thorne, P.D., Vincent, C.E., 1995. Backscattering from a suspension in the nearfield of a piston transducer. J. Acoust. Soc. Am. 97, 1614–1620.

Flammer, G.H., 1962. Survey Ultrasonic measurement of suspended sediment. U.S. Geological Bulletin 1141-A. Government Printing Office, Washington, DC, 48 pages.

Gaunaurd, G. C., and Uberall, H. 1983. RST analysis of monostatic and bistatic acoustic echoes from an elastic sphere. J. Acoust. Soc. Am. 73(1), 1–12.

Gitto, A. (2015). Representative point integrated suspended sediment sampling in rivers. M.Sc. thesis. Simon Fraser University, BC, Canada.

Guerrero M., Szupiany, R.N. and Latosinski, F. 2013. Multi-frequency acoustics for suspended sediment studies: an application in the Parana River. Journal of Hydraulic Research, 51:6, 696-707,

Haught, D.W., Venditti, J. and Church, M. 2014. Acoustic sediment flux observations on the Fraser River, Canada. In River Flow 2014 ed A.J. Schleiss, G. de Cesare, M.J. Franca and M. Pfister (London: CRC Press) 1943-1950

Hay, A.E., 1991. Sound scattering from a particle-laden, turbulent jet. J. Acoust. Soc. Am. 90, 2055-2074.

Hay, A.E., and Sheng, J., 1992. Vertical profiles of suspended sand concentration and size from multifrequency acoustic backscatter. J. Geophys. Res. 97, 15661-15677.

Holdaway, G.P., Thorne, P.D., Flatt, D., Jones, S.E., Prandle, D. 1999. Comparison between ADCP and transmissometer measurements of suspended sediment concentration. Cont. Shelf Res.19,421–441.

MacDonald, I. T., Vincent, C. E., Thorne, P. D. and Moate, B. D. 2013. Acoustic scattering from a suspension of flocculated sediments, J. Geophys. Res. Oceans, 118, 2581-2594.

McLean, D. G., Church, M., & Tassone, B. 1999a. Sediment transport along lower Fraser River: 1. Measurements and hydraulic computations. Water Resources Research, 35(8), 2533.

McLean, D.G. and Church, M. 1999b. Sediment transport along lower Fraser River. 2. Estimates based on the long-term gravel budget. Water Resources Research, 35, 2549-2559.

Moate, B.D. and Thorne, P.D., 2009. Measurements and inversion of acoustic scattering from suspensions having broad size distributions. J. Acoust. Soc. Am., 126, 2905-2917.

Moate, B.D., Thorne, P.D. 2011. Interpreting acoustic backscatter from suspended sediments of different and mixed mineralogical composition. Cont. Shelf Res., 46, 67–82.

Moate B.D. and Thorne P.D. 2013. Scattering from suspended sediments having different and mixed mineralogical compositions: Comparison of laboratory measurements and theoretical predictions. J. Acoust. Soc. Am., 133 (3).

Moore, S.A., Le Coz, J., Hurther, D., and Paquier, A., 2012. On the application of horizontal ADCPs to suspended sediment transport surveys in rivers. Cont. Shelf Res., 46, 50-63.

Moore S.A., Le Coz J., Hurther, D., Paquier A. 2013. Using multi-frequency acoustic attenuation to monitor grain size and concentration of suspended sediment in rivers. J. Acoust. Soc. Am. 133 (4).

Richards, S.D., Leighton, T.G., and Brown, N.R., 2003. Visco-inertial absorption in dilute suspensions of irregular particles. Proceedings of the Royal Society of London 459, 2153-2167.

Schaafsma, A.S., Hay, A.E., 1997. Attenuation in suspensions of irregularly shaped sediment particles: a two-parameter equivalent spherical scatterer model. J. Acoust. Soc. Am. 102 (3), 1485–1502.

Sheng, J., and Hay, A.E., 1988. An examination of the spherical scatterer approximation in aqueous suspensions of sand. J. Acoust. Soc. Am. 83(2), 598-610.

Teledyne RD Instruments. 2008. Workhorse H-ADCP Operational Manual. pp. 87, 158.

Thorne, P. D., Agrawal, Y. C., Cacchione, D.A. 2007. A comparison of near-bed acoustic backscatter and laser diffraction measurements of suspended sediments. IEEE J. Ocean Eng. 32(1), 225–235.

Thorne, P.D. and Buckingham, M.J. 2004. Measurements of scattering by suspensions of irregularly shaped sand particles and comparison with a single parameter modified sphere model. J. Acoust. Soc. Am. 116(5), 2876-2889.

Thorne, P. D., and Campbell, S. C. 1992. Backscattering by a suspension of spheres. J. Acoust. Soc. Am. 92, 978–986.

Thorne, P.D., and Hanes, D.M., 2002. A review of acoustic measurements of small-scale sediment processes. Cont. Shelf Res., 22, 603-632.

Thorne, P.D. and Hardcastle, P.J., 1997. Acoustic measurement of suspended sediments in turbulent currents and comparison with in-situ samples. J. Acoust. Soc. Am.101(5), 2603-2614.

Thorne, P.D., Hardcastle, P.J., Flatt, D., Humphery, J.D. 1994. On the use of acoustics for measuring shallow water suspended sediment processes. IEEE J. Oceanic Eng. 19 (1), 48–57.

Thorne, P. D. and Hurther, D. 2014. An overview on the use of backscattered sound for measuring suspended particle size and concentration profiles in non-cohesive inorganic sediment transport studies. Cont. Shelf Res., 73, 97-118.

Thorne P.D., MacDonald I.T., and Vincent C.E. 2014. Modelling acoustic scattering by suspended flocculating sediments. Cont. Shelf Res., Volume 88, 1, Pages 81-91.

Thorne, P.D. and Meral, R. 2008. Formulations for the scattering properties of suspended sandy sediments for use in the application of acoustics to sediment transport processes. Cont. Shelf Res., 28, 309-317.

Thorne, P.D., Waters, K.R., Brudner, T.J., 1995a. Acoustic measurements of scattering by objects of irregular shape. Journal of the Acoustical Society of America 97 (1), 242–251.

Thosteson, E. D., Hanes, D. M. 1998. A Simplified method for determining sediment size and concentration from multiple frequency acoustic backscatter measurements. J. Acoust. Soc. Am. 104(2), 820–830. (Pt.1).

Topping, D.J., Rubin, D.M., Wright, S.A., and Melis, T.S. 2011. Field evaluation of the error arising from inadequate time averaging in the standard use of depth-integrating suspended-sediment samplers. U.S. Geological Survey Professional Paper 1774, 95 p.

Urick, R.J., 1948. The absorption of sound in suspensions of irregular particles. J. Acoust. Soc. Am. 20(3), 283-289.

Urick R.J., 1975. Principles of Underwater Sound for Engineers, New York: McGraw Hill, 384 p.

Walling, D.E., 1977. Assessing the accuracy of suspended sediment rating curves for a small basin. Water Resources Research 12, 1869–1894.